The Impact of Transmission Line and Grounding System Modeling on Special Lightning Protection Systems ⋆

Jaimis S. L. Colqui * **Rodolfo A. R. Moura** ** **Marco Aurélio O. Schroeder** ** **José Pissolato Filho** *

* *School of Electrical and Computer Engineering, State University of Campinas, Brazil (e-mail: jaimis@unicamp.br; pisso@unicamp.br)*
** *Electrical Engineering Department, Federal University of São João del-Rei, Brazil (e-mail: moura@ufsj.edu.br; schroeder@ufsj.edu.br)*

Abstract: This paper aims to assesses the performance of different models of transmission lines and grounding systems when using the underbuilt-wire protection technique against lightning overvoltages. Moreover, the frequency dependence of the soil parameters is also investigated. A first stroke representative waveform of lightning current is considered and the simulations took place in the Alternative Transients Program (ATP). It was found that simplified models of transmission lines and grounding systems that consider constant frequency electrical ground parameters result in inaccurate responses of overvoltages in the insulator strings. According to the results, depending on the case, maximum differences of 20.23% can be found.

Keywords: Lightning protection; transmission line modeling; underbuilt wire; grounding system modeling; back-flashover; time-domain simulations.

1. INTRODUCTION

Lightning is one of the main causes of fault in transmission lines. The lightning-caused failure of the transmission line can be, basically, divided into three mechanism [1]: i) flashover - due to lightning striking directly the phase conductors; ii) back-flashover - due to lightning striking either the top of the tower or the ground-wires; iii) and mid-span flashover - can occur in particular situations where the spans are too long, leading to a possible flashover that may connect the shield wires and phase conductors through the air (Visacro et al., 2012; Silveira et al., 2012). Among these mechanism, usually, back-flashover is the main cause of shutdown. Hence, the transient analysis of transmission lines, particularly direct lightning strike, is essential to estimate the back-flashover rates, therefore, reliability, insulation coordination investigation, optimization of insulator string length and optimization of tower structure (Asadpourahmadchali et al., 2020).

The occurrence of back-flashover depends on the physical characteristics of the insulator that supports the line and its ability to withstand certain voltage waveforms and magnitudes (Martínez, 2010). Moreover, the local characteristics have a direct influence on the performance of the lines, such as the impulse impedance of the grounding system, the soil resistivity, the density of atmospheric discharges in the region, among others, since this parameters can influency the overvoltage across insulator strings. In some specific cases, the lines may be located in regions with high resistivity soils, which results in inefficient grounding systems and/or in regions with a high density of lightning, which increases the susceptibility of the system to the occurrence of shutdown (Visacro et al., 2012).

To minimize the influence of these conditions and improve lightning performance, there are protection techniques, such as line arresters (Visacro et al., 2020), installation of additional shield wire (Banjanin, 2018), installation of underbuilt shield wires (Silveira et al., 2012; Banjanin, 2018; Batista et al., 2021) and application of guy wires on overhead line towers (Banjanin, 2018).

The installation underbuilt wires is an unusual protection technique and can be used, due to the mentioned characteristics, to reduce the failure rate. This method consists of installing one or more shield wire conductors below the phase conductors, being connected to the tower and its grounding system. Installation can be done only in adjacent spans of a tower with critical performance or in sections of a line with high failure rates (Visacro et al., 2012).

This technique proves to be a potential alternative for reducing overvoltages originating from lightning (Banjanin, 2018; Visacro et al., 2020; CIGRE Working Group C4.23, 2021), due to advances in modeling of transmission line components and the use of modern simulation tools, a study of the performance of the influence of line components and the grounding system on lightning overvoltages is required.

⋆ This work was supported by São Paulo Research Foundation (FAPESP) (grant: 2021/06157-5).

[1] since this work only consider transmission lines, it is considered that the electrical field generated in the insulator strings due to indirect lightning, i.e., lightning that does not strike the system directly, are not capable of disrupt the insulator strings.

The rigorous representation of the transmission line and grounding system for impulsive currents is of utmost importance to obtain accurate and consistent results of transmission lines performance. In the last decade, several studies have shown the importance of considering the variation of soil resistivity and permittivity with frequency in the assessment of the impulse behavior of counterpoise cables (Schroeder et al., 2018) and transmission lines (Alípio et al., 2019; De Conti and Emídio, 2016; Colqui et al., 2021).

This work presents a comparison of the overvoltages along the insulator strings due to the injection of a lightning current waveform. For this, the use of different models of transmission lines and grounding systems was considered. Moreover, it is also verified the impact of assuming the frequency dependence of soil parameters. Therefore, an attempt is made in this paper to show possible inaccuracies associated with the assumption of constant ground parameters and simplifications of the models in the simulation of lightning transients in transmission lines.

The remaining sections of the paper are organized as follows: Section 2 the modeling details and simulated systems are presented, in Section 3 the results are presented and analyzed, and in Section 4 presents the major conclusions of this paper.

2. SYSTEM DESCRIPTION

In order to assess the impact of transmission line (TL) and grounding system modeling in the special lightning protection system, three towers and four spans of a 138-kV line were considered. The results are obtained considering the lightning striking the central tower. To avoid unrealistic reflections, aerial conductors were impedance matched 400 m away from the adjacent towers. The silhouette of the tower and the line cable heights are illustrated in Fig. 1(a), where the values within parenthesis are midspan heights. This TL is composed by the phase conductors (A, B and C), one ground wires (GW) and one underbuilt wire (UW) shown in Table 1. Fig. 1(b) shows the typical grounding arrangement of the studied transmission towers. It consists of 4 counterpoise cables and each one starting from a tower foot.

The modeling of each component are briefly described hereafter.

2.1 Frequency Dependence of Soil Parameters

Different models that take into account the frequency dependence of soil parameters can be found in literature (Cavka et al., 2014). These models are expressed in terms of curve-fitting equations for the soil conductivity and relative permittivity, which are based on laboratorial or in-situ experimental data. In this paper, the Alipio-Visacro model (Alípio and Visacro, 2014) is considered. This model satisfies causality, it was obtained considering in-situ experiments and was recently recommended by CIGRE Working Group C4.33 (2019) for lightning-related studies. In (1) and (2) illustrate the formulation of the model.

$$\sigma_g(f) = \sigma_0 + \sigma_0 \times h(\sigma_0)\left(\frac{f}{1\text{MHz}}\right)^{\xi} \quad (1)$$

$$\varepsilon_{rg}(f) = \varepsilon_{r\infty} + \frac{\tan(\pi\xi/2) \times 10^{-3}}{2\pi\varepsilon_0(1\text{MHz})^{\xi}}\sigma_0 \times h(\sigma_0)f^{\xi-1} \quad (2)$$

where σ_g is the soil conductivity in [mS/m] (or resistivity $\rho_g = \sigma_g^{-1}$), σ_0 is the DC conductivity in [mS/m], ε_{rg} is the relative permittivity in [F/m], $\varepsilon_{r\infty}$ is the relative permittivity at higher frequencies, ε_0 is the vacuum permittivity in [F/m] and f is the frequency in [Hz]. According to Alípio and Visacro (2014), the following parameters are recommended in (1) and (2) to obtain mean results for the frequency variation of σ_g and ε_{rg} : $\xi = 0.54$, $\varepsilon_{r\infty} = 12$ and $h(\sigma_0) = 1.26 \,\text{x}\, \sigma_0^{-0.73}$.

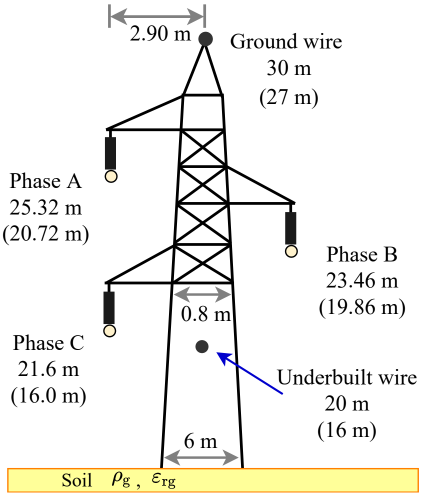

(a)

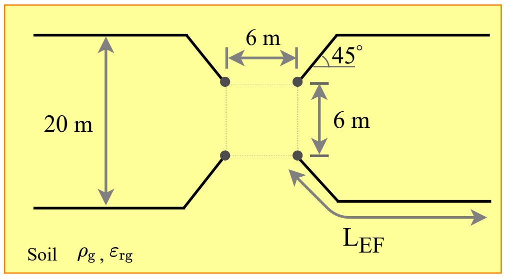

(b)

Figure 1. (a) Tower silhouette and (b) Arrangement of tower-footing grounding electrodes.

Table 1. Conductors applied to the 138-kV TL.

Phase cables: ACSR (1 conductor/phase)			
Phases	rint (cm)	rext (cm)	R(Ω/km)
A	-	1.60	0.063
B	-	1.60	0.063
C	-	1.60	0.063
GW and UW: 3/8" EHS (1 conductor/phase)			
GW	-	0.79	0.500
UW	-	0.79	0.500

2.2 Transmission Line Model

Two models are adopted in this paper to represent the TL. The first is the JMarti model (Marti, 1982), which represents the line with distributed electrical parameters and emulates the TL parameters frequency dependence over a pre-defined frequency range (Dommel, 1969). The configuration of JMarti model available in the ATP software considers Carson's equations for calculating the ground return impedance of TLs and a Bode's method for synthesize the characteristic impedance $\boldsymbol{Z_c}$ and propagation function $\boldsymbol{H}$ matrices (Prikler and Hoidalen, 2009). These equations disregard the frequency dependence of the soil electrical parameters and neglect displacement currents in the ground return impedance calculation.

In order to evaluate the effect of frequency dependent soil parameters in the simulation of lightning overvoltages on overhead transmission lines, a second model, here called modified Marti's model (De Conti and Emídio, 2016), is used. The implementation of modified Marti's model employ the Vector Fitting method (Gustavsen and Semlyen, 1999) to fit the matrices $\boldsymbol{Z_c}$ and $\boldsymbol{H}$, the line parameters are computed using the Carson's model (Carson, 1926) or Sunde's model (Sunde, 1968). This implementation can also include the frequency dependence of soil parameters in the calculation of the ground return impedance, assuming the soil parameters to vary as described in (1) and (2). The ground admittance, was calculated considering the soil as a perfect electrical conductor, because the soil has a negligible effect on transients in overhead lines, considering the frequency range of interest in this work (Alípio et al., 2019).

In this paper, the Sunde's equations (which can be expressed by replacing k by 0 in (5)) and Carson's equations (which can be expressed by replacing k by ε_{rg} in (5)) is used, similarly as proposed in De Conti and Emídio (2016). Hence, the ground-return impedance is calculated considering Equations (3) and (4).

$$Z_{g_{\mathrm{ii}}}(f) = j\frac{\omega\mu_0}{\pi}\int_0^{\infty}\frac{e^{-2h_{\mathrm{i}}\lambda}}{\sqrt{\lambda^2+\gamma_{\mathrm{g}}^2}+\lambda}d\lambda \tag{3}$$

$$Z_{g_{\mathrm{ij}}}(f) = j\frac{\omega\mu_0}{\pi}\int_0^{\infty}\frac{e^{-(h_{\mathrm{i}}+h_{\mathrm{j}})\lambda}}{\sqrt{\lambda^2+\gamma_{\mathrm{g}}^2}+\lambda}\cos(r_{\mathrm{ij}}\lambda)d\lambda \tag{4}$$

where

$$\gamma_g = \sqrt{j\omega\mu_0(\sigma_{\mathrm{g}} + j\omega(\varepsilon_{rg}-k)\varepsilon_0)} \tag{5}$$

in which $\omega = 2\pi f$ is the angular frequency in [rad/s], f is the frequency in [Hz], μ_0 is the vacuum permittivity in [H/m], ε_0 is the vacuum permittivity in [F/m], ε_{rg} is the relative permittivity, σ_{g} is the soil conductivity in [S/m], r_{ij} is the horizontal separation between conductors i and j in [m], h_i and h_j are the heights of conductors i and j above the soil in [m].

2.3 Tower Model

The tower is commonly modeled using the transmission line theory by means of one or more sections of a lossless single-phase transmission line (Piantini, 2020). The representation of the tower through a single section (or segment) is not able to represent the variations in the geometry of the structure along its height (De Conti et al., 2006). One technique, widely used in the literature, consists of representing the tower through several sections, each one being represented by a lossless single-phase line. The surge impedances of each section are calculated using the revised Jordan's formula proposed in De Conti et al. (2006), which take into account vertical multiconductor systems. The methodology allows the calculation of the self and mutual surge impedances of vertical multiconductor systems leading to a simplified representation of towers using the theory of transmission lines. The self surge impedance of a single vertical conductor is obtained by (6) and the mutual surge impedance of vertical conductors by (7) (De Conti et al., 2006).

$$Z_{ii} = 60\ln\left(\frac{4h}{r}\right) - 60 \tag{6}$$

$$Z_{ij} = 60\ln\frac{2h+\sqrt{4h^2+d_{ij}^2}}{d_{ij}} + 30\frac{d_{ij}}{h} - 60\sqrt{1+\frac{d_{ij}^2}{4h^2}} \tag{7}$$

where h is the height of the conductor, r is the conductor radius, and d_{ij} corresponds to the distance between the centers of conductor i and j.

If the n vertical conductors of a transmission line tower are connected at the current injection point, the whole system can be represented as a single transmission line with equivalent surge impedance given by

$$Z_{eq(i)} = \frac{Z_{i1}+Z_{i2}+\cdots+Z_{ii}+\cdots+Z_{in}}{n} \tag{8}$$

In this case, $n = 4$ and the equivalent impedance of each tower segment was computed using (6)–(8), considering average spaces between tower conductors and the heights. Fig. 2 shows the obtained results. Note each tower section is represented by single surge impedance, although a single equivalent surge impedance could be obtained. The propagation velocity of the waves in the tower is considered equal to 80% of the speed of light in the vacuum (De Conti et al., 2006).

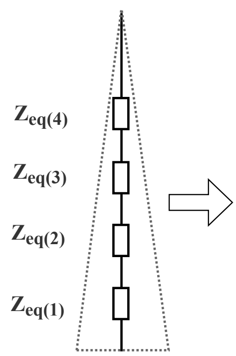

ATP/EMTP:
4 TLs with surge impedances

	Z_{eq} (Ω)	v (m/s)
(1)	201.5511	2.4×10^8
(2)	268.4276	2.4×10^8
(3)	272.6594	2.4×10^8
(4)	304.7648	2.4×10^8

Figure 2. Transmission tower model.

2.4 Insulator Strings

The insulation strength depends on the waveform of the applied voltage. Considering lightning, to determine whether or not the line insulation breakdown may be evaluated using the following approaches:

- Voltage–time curves (Imece et al., 1996);
- Disruptive effect method (Witzke and Bliss, 1950);
- Physicals models (Pigini et al., 1989; Banjanin and Savić, 2016).

In this work, it has been adopted the Disruptive effect method (DE method) approach, since it is easy to obtain its parameters and it also presents an excellent accuracy (Hileman, 1999).

The DE method concept is based on the idea of the existence of a critical disruptive effect DE_C for each insulator configuration. Each non-standard voltage surge has an associated disruptive effect (DE). If this DE value exceeds the critical value, a disruptive discharge occurs, which causes the insulation to break (Hileman, 1999). The disruptive effect associated with a voltage waveform is determined by

$$DE = \int_{t_0}^{t_a} \left(v(t) - V_0\right)^k dt \tag{9}$$

where $v(t)$ corresponds to the voltage waveform applied over the insulator string, V_0 refers to the voltage threshold from which it has begun the process of rupture in the insulator, t_0 is the instantaneous value of $v(t)$ exceeds V_0, k is a dimensionless factor, and DE is the variable called "disruptive effect". For a typical 138-kV line, DE method constants can be obtained according to Hileman (1999): $DE_c = 1.1506\,(CFO)^k$; $k = 1.36$; $V_0 = 0.77\,CFO = 500.5$ kV.

2.5 Tower-footing Grounding

The tower-footing grounding system plays a fundamental role in back-flashover occurrence when the shield wire and the tower are subjected to direct strikes. To calculate the grounding impedance, three different methodologies were considered. The first represents the grounding system by a simple resistance equal to the resistance of low frequency grounding (R_{LF}), the second and third use the Hybrid Electromagnetic Model (HEM) with constant or frequency dependent electrical parameters of the soil, respectively.

For the second and third methodology the impedance $Z(\omega)$ of the tower-footing grounding is determined using the accurate HEM (Visacro and Soares, 2005), in a frequency range from DC to several MHz. As detailed Visacro and Soares (2005), the HEM solves Maxwell's equations numerically via the vector and scalar potentials using the thin wire approximations. In the calculations, the frequency dependence of the soil parameters is taken into account using (1) and (2). After determining the harmonic impedance $Z(\omega)$, a pole-residue model of the associated admittance $Y(\omega)$=1/$Z(\omega)$ is obtained using the vector fitting (VF) method (Gustavsen and Semlyen, 1999). Finally, an electrical network that is suitable to time-domain simulations is determined from the passive pole residue model corresponding to the grounding admittance. Both the pole-residue model and the electrical network were obtained using the VF method (Gustavsen and Semlyen, 1999).

2.6 Lightning Current

A proper evaluation of lightning effects on power systems relies upon, among other factors, on an appropriate representation of the lightning current waveform since the quality of the simulation results depends on the representative of the assumed lightning current waves. According to Visacro et al. (2004), the first stroke currents are characterized by a pronounced concavity at the front and by the occurrence of multiple peaks, being the second peak usually the highest one, and the maximum steepness occurring near the first peak according to measurements of instrumented towers, such as those presented in Visacro et al. (2004). Considering the previous aspects, the simulations were performed considering some Brazilian conditions that approximately reproduces the main median parameters of first strokes measured at Morro do Cachimbo Station. As detailed in De Conti and Visacro (2007), the waveform of lightning is obtained by a sum of Heidler functions described in (10) and (11).

$$i(t) = \sum_{k=1}^{N} \frac{I_{0k}}{\eta_k} \frac{\left(t/\tau_{1k}\right)^{n_k}}{1 + \left(t/\tau_{1k}\right)^{n_k}} \exp^{(-t/\tau_{2k})} \tag{10}$$

$$\eta_k = \exp\left[-\left(\frac{\tau_{1k}}{\tau_{2k}}\right)\left(n_k\frac{\tau_{2k}}{\tau_{1k}}\right)^{\frac{1}{n_k}}\right] \tag{11}$$

where I_{0k} controls the amplitude, τ_{1k} is the time constant associated with the front time, τ_{2k} is the decay time constant, η_k is the factor of correction of the amplitude and n_k is the exponent which controls the inclination of each component k added to build $i(t)$.

Since for direct lightning-related studies, first strokes are the most nefarious, since it has more intense peak values, in this paper only the first stroke currents will be considered. The statistics of measurements performed at the Morro do Cachimbo Station are used (Visacro et al., 2004). To obtain the current waveforms, each parameter of (10) and (11) is adjusted taking as reference the median characteristics of first stroke currents and the multiplier α on the current waveform, as detailed in Oliveira et al. (2017).

3. RESULTS

This section presents the results of the simulation of overvoltages obtained in an event of a lightning striking the central tower. At first, to analyze the impact of using the under-built wires, Figs. 3(a), 3(b) and 3(c) illustrate the lightning overvoltage at the top of the tower for lines with or without the under-built, considering the soil resistivities of 1000 Ω.m, 3000 Ω.m and 10000 Ω.m. The reduction in lightning overvoltages peaks using the installation of underbuilt shield wires cables was of 3.384%, 5.540% and 8.681%, respectively. In this case, it was considered the JMarti model, already implemented in the ATP, and the grounding model was considered the R_{LF}.

In order to compare the aforementioned models (transmission line and grounding), Table 2 summarizes five different representations, deliberately chosen, of the transmission system models. These representations were set to be used in the simulations. Also, the low-frequency soil resistivities considered are: 1000, 3000 and 10000 Ω.m. For these resistivities, it was considered the effective length, obtained by using ref CIGRE Working Group C4.23 (2021). The effective length and low frequency resistance of the counterpoise cable are shown in Table 3.

The multiplier α (which changes the amplitude of the mean lightning current curve measured in the Morro do Cachimbo Station) used for the resistivities of 1000, 3000 and 10000 Ω.m was 0.8, 3.75 and 2.85, respectively. These values were chosen randomly and in order to represent currents that generate back-flashover in some of the phases for the simulations with resistivities 3000 Ω.m and 10000 Ω.m.

ISSN: 2177-6164

DOI: 10.20906/sbse.v2i1.2918

Table 2. Types of modeling representations.

Rep.	TL model	Appro.	Soil for TL	Ground. model
1	JMarti	Carson	ρ_0	R_{LF}
2	JMarti	Carson	ρ_0	Z (ρ_0, ε_r)
3	Modified Marti's	Carson	ρ_0	Z (ρ_0, ε_r)
4	Modified Marti's	Sunde	$\rho(\omega)$, $\varepsilon_r(\omega)$	Z (ρ_0, ε_r)
5	Modified Marti's	Sunde	$\rho(\omega)$, $\varepsilon_r(\omega)$	Z ($\rho(\omega)$, $\varepsilon_r(\omega)$)

Table 3. Length of the counterpoise wires and R_{LF} values as a function of soil resistivity.

	ρ_0=1000 Ω.m	ρ_0=3000 Ω.m	ρ_0=10000 Ω.m
L_{EF} [m]	55	100	180
R_{LF} [Ω]	11.9	22.3	46.5

Figs. 4, 5 and 6 illustrate the overvoltages (across insulator strings of phases A, B and C of the 138-kV line), considering the various representations shown in Table 2 and and the soil resistivities of 1000 Ω.m, 3000 Ω.m and 10000 Ω.m.

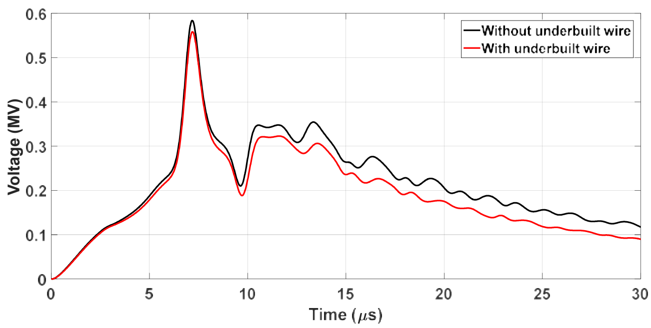

(a)

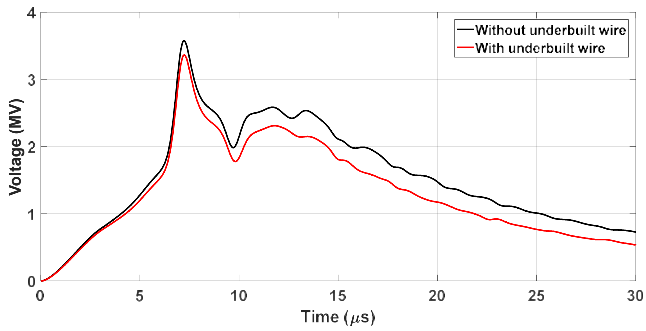

(b)

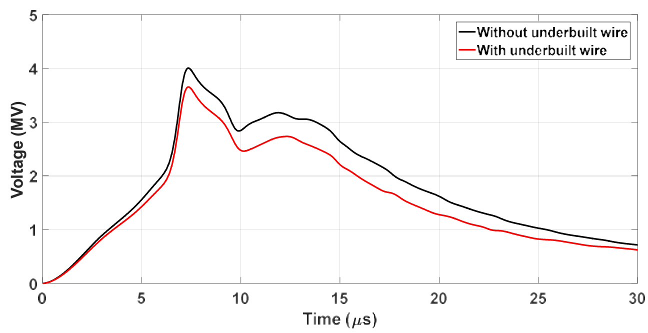

(c)

Figure 3. Reduction of overvoltage at the shield wire of the line due to the use of underbuilt cables, considering soil with; (a) ρ_0=1000 Ω.m, (b) ρ_0=3000 Ω.m and (c) ρ_0=10000 Ω.m.

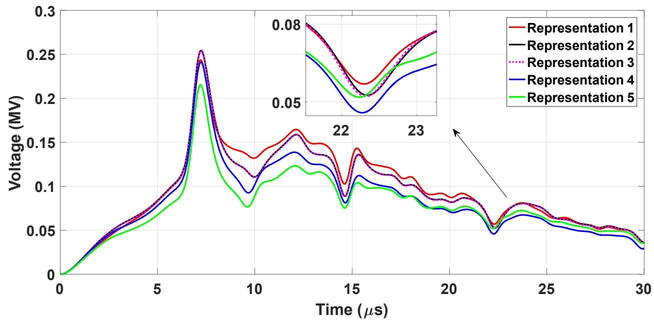

(a)

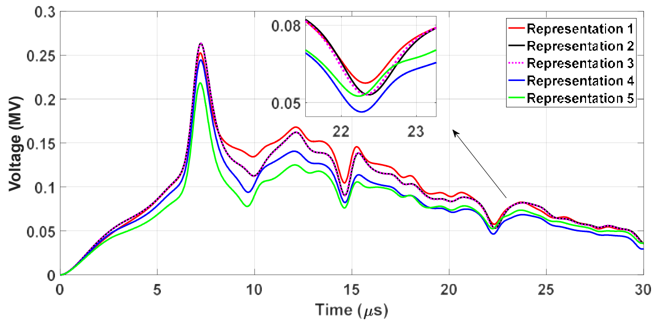

(b)

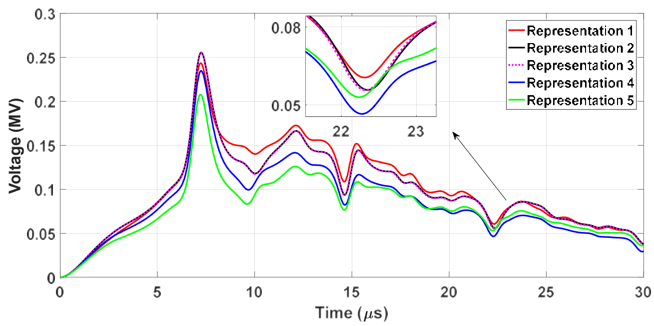

(c)

Figure 4. Overvoltages across the insulator string of the line, considering soil with ρ_0=1000 Ω.m; (a) Phase A, (b) Phase B and (c) Phase C.

In the case of Fig. 4, it can be observed that for all representations the back-flashover phenomenon does not occur in any of the phases of the line. Also, at the peaks of the overvoltages in representations 1, 2, 3 and 4 present maximum differences of 16.94%, 20.23%, 20.23% and 14.4% in relation to representation 5, which is the most complete representation. On the other hand, the peak of the overvoltages in representations 2 and 3 are almost equal and the peak in representation 1 and 4 are close to the previous representations.

In the case of Fig. 5, it can be observed that only in phases B and C of the line in representations 2 and 3, and phase B in representation 4 does the phenomenon of back-flashover occur and that in other representations it does not occur. This is because representations 2 and 3 is the representation of the simplest models, and the most conservative. Also, at the peaks of the overvoltages in representations 1, 2, 3 and 4 they present maximum differences of 13.16%, 14.21%, 14.21% and 13.72% in relation to representation 5, which is the most complete representation. On the other hand, similar to the analysis for Fig. 4, the overvoltages

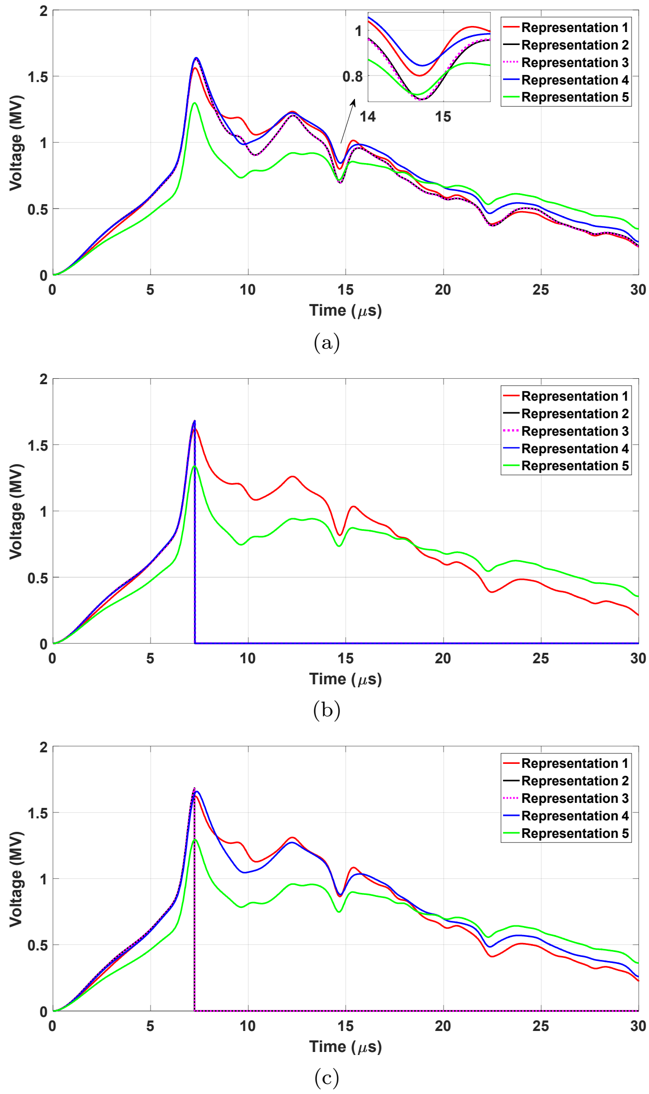

Figure 5. Overvoltages across the insulator string of the line, considering soil with ρ_0=3000 Ω.m; (a) Phase A, (b) Phase B and (c) Phase C.

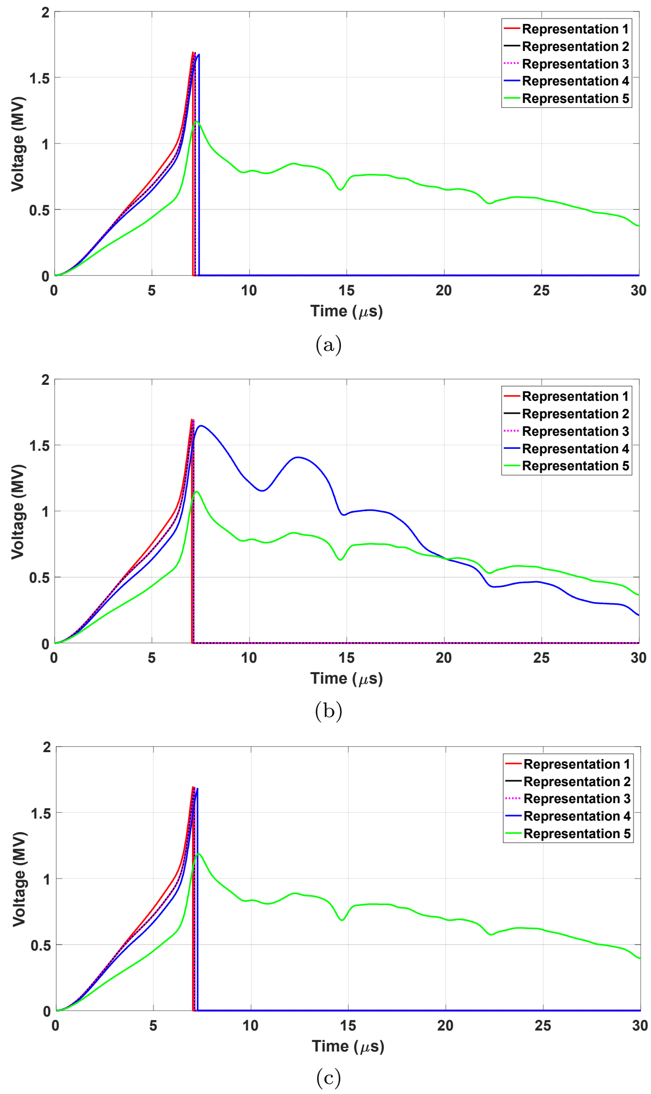

Figure 6. Overvoltages across the insulator string of the line, considering soil with ρ_0=10000 Ω.m; (a) Phase A, (b) Phase B and (c) Phase C.

peak in phase C for representations 2 and 3 are almost equal.

In the case of Fig. 6, it can be observed that in phases A and C of the line in representations 1, 2, 3 and 4, the phenomenon of back-flashover occurs, and for representation 5 it does not occur. In phase B of the line, representations 1, 2 and 3 also occur the phenomenon of back-flashover, which in representations 4 and 5 does not occur.

The analysis considered different representations of the models of transmission lines and grounding systems in the special lightning protection system to calculate the overvoltages in the transmission line. As shown in this section, when using simplified models (representations 1, 2, 3 and 4) to evaluate back-flashover calculations, for example, the results can be erroneous and therefore it is preferable to use more accurate representations (representation 5), which take into account the frequency dependence of the electrical parameters of the ground.

4. CONCLUSIONS

This paper investigates the influence of considering frequency dependent soil parameters in transmission line and grounding system models when using the protection technique against lightning overvoltages well-known as under-built wire. According to results, there are relevant differences in considering the frequency dependence of the soil in grounding modeling. However, these difference is negligible when considering the frequency dependence of the soil in transmission line modeling.

Moreover, these differences became more pronounced with increasing the value of the soil resistivity and might be important in determining the line back-flashover. Overall, if accurate estimates of the lightning performance of a transmission line are required, the frequency dependence of soil parameters should be incorporated on grounding system models, especially for high resistivity soils.

It is worth mentioning that the results presented in this paper correspond to overvoltages developed along the in-

ISSN: 2177-6164 DOI: 10.20906/sbse.v2i1.2918

sulator strings due to first stroke lightnings, i.e., relatively slow front time. Hence, for the cases when the currents have a shorter front time, due to the higher frequency content of the current, the differences observed between the voltage waveforms calculated assuming or neglecting the variation of the soil parameters with frequency may be more pronounced.

REFERENCES

Alípio, R.S., De Conti, A., Miranda, A., and Correia De Barros, M.T. (2019). Lightning Overvoltages Including Frequency-Dependent Soil Parameters in the Transmission Line Model. In *Proceedings of the International Conference on Power Systems Transients (IPST)*. Perpignan, France.

Alípio, R.S. and Visacro, S. (2014). Modeling the frequency dependence of electrical parameters of soil. *IEEE Transactions on Electromagnetic Compatibility*, 56(5), 1163–1171.

Asadpourahmadchali, M., Niasati, M., and Alinejad-Beromi, Y. (2020). Improving tower grounding vs. insulation level to obtain the desired back-flashover rate for hv transmission lines. *International Journal of Electrical Power Energy Systems*, 123, 106171.

Banjanin, M.S. (2018). Application possibilities of special lightning protection systems of overhead distribution and transmission lines. *International Journal of Electrical Power Energy Systems*, 100, 482–488.

Banjanin, M.S. and Savić, M.S. (2016). Some aspects of overhead transmission lines lightning performance estimation in engineering practice. *International Transactions on Electrical Energy Systems*, 26(1), 79–93.

Batista, R., Louro, P.E., and Paulino, J.O. (2021). Lightning performance of a critical path from a 230-kV transmission line with grounding composed by deep vertical electrodes. *Electric Power Systems Research*, 195, 107165.

Carson, J.R. (1926). Wave Propagation in Overhead Wires with Ground Return. *Bell System Technical Journal*, 5(4), 539–554.

Cavka, D., Mora, N., and Rachidi, F. (2014). A Comparison of frequency-dependent soil models: Application to the analysis of grounding systems. *IEEE Transactions on Electromagnetic Compatibility*, 56(1), 177–187.

CIGRE Working Group C4.23 (2021). Procedures for Estimating the Lightning Performance of Transmission Lines – New Aspects.

CIGRE Working Group C4.33 (2019). Impact of soil-parameter frequency dependence on the response of grounding electrodes and on the lightning performance of electrical systems.

Colqui, J.S.L., Araújo, A.R.J., Pascoalato, T.F.G., and Kurokawa, S. (2021). Transient analysis of overhead transmission lines based on fitting methods. In *2021 14th IEEE International Conference on Industry Applications (INDUSCON)*, 180–187.

De Conti, A. and Emídio, M.P.S. (2016). Extension of a modal-domain transmission line model to include frequency-dependent ground parameters. *Electric Power Systems Research*, 138, 120–130.

De Conti, A. and Visacro, S. (2007). Analytical representation of single- and double-peaked lightning current waveforms. *IEEE Transactions on Electromagnetic Compatibility*, 49(2), 448–451.

De Conti, A., Visacro, S., Soares, A., and Schroeder, M.A.O. (2006). Revision, extension, and validation of Jordan's formula to calculate the surge impedance of vertical conductors. *IEEE Transactions on Electromagnetic Compatibility*, 48(3), 530–536.

Dommel, H.W. (1969). Digital Computer Solution of Electromagnetic Transients in Single-and Multiphase Networks. *IEEE Transactions on Power Apparatus and Systems*, PAS-88(4), 388–399.

Gustavsen, B. and Semlyen, A. (1999). Rational approximation of frequency domain responses by vector fitting. *IEEE Transactions on Power Delivery*, 14(3), 1052–1061.

Hileman, A.R. (1999). *Insulation Coordination for Power Systems*. CRC Taylor Francis.

Imece, A.F., Durbak, D.W., Elahi, H., Kolluri, S., Lux, A., Mader, D., McDermott, T.E., Morched, A., Mousa, A.M., Natarajan, R., and Rugeles, L. (1996). Modeling guidelines for fast front transients. *IEEE Transactions on Power Delivery*, 11(1), 493–501.

Marti, J.R. (1982). Accurate Modeling of Frequency-Dependent Transmission Lines in Electromagnetic Transient Simulations. *IEEE Power Engineering Review*, 2(1), 29–30.

Martínez, J.A.V. (2010). *Power System Transients: Parameter Determination*. CRC Press.

Oliveira, A.J., Schroeder, M.A.O., Moura, R.A., De Barros, M.T.C., and Lima, A.C. (2017). Adjustment of current waveform parameters for first lightning strokes: Representation by Heidler functions. *2017 International Symposium on Lightning Protection, XIV SIPDA 2017*, 121–126.

Piantini, A. (2020). *Lightning Interaction with Power Systems - Volume 1: Fundamentals and Modelling*. Institution of Engineering and Technology.

Pigini, A., Rizzi, G., Garbagnati, E., Porrino, A., Baldo, G., and Pesavento, G. (1989). Performance of large air gaps under lightning overvoltages: experimental study and analysis of accuracy predetermination methods. *IEEE Transactions on Power Delivery*, 4(2), 1379–1392.

Prikler, L. and Hoidalen, H. (2009). ATPDraw version 5.6 manual. *European EMTP ATP Users Group*.

Schroeder, M.A.O., de Barros, M.T.C., Lima, A.C., Afonso, M.M., and Moura, R.A. (2018). Evaluation of the impact of different frequency dependent soil models on lightning overvoltages. *Electric Power Systems Research*, 159, 40–49.

Silveira, F.H., Visacro, S., De Conti, A., and De Mesquita, C.R. (2012). Backflashovers of transmission lines due to subsequent lightning strokes. *IEEE Transactions on Electromagnetic Compatibility*, 54(2), 316–322.

Sunde, E.D. (1968). *Earth conduction effects in transmission systems*. Dover Publications, New York.

Visacro, S. and Soares, A. (2005). HEM: A model for simulation of lightning-related engineering problems. *IEEE Transactions on Power Delivery*, 20(2 I), 1206–1208.

Visacro, S., Silveira, F.H., and De Conti, A. (2012). The use of underbuilt wires to improve the lightning performance of transmission lines. *IEEE Transactions on Power Delivery*, 27(1), 205–213.

Visacro, S., Silveira, F.H., Pereira, B., and Gomes, R.M. (2020). Constraints on the use of surge arresters for improving the backflashover rate of transmission lines. *Electric Power Systems Research*, 180, 106064.

Visacro, S., Soares Jr, A., Schroeder, M.A.O., Cherchiglia, L.C., and de Sousa, V.J. (2004). Statistical analysis of lightning current parameters: Measurements at Morro do Cachimbo Station. *Journal of Geophysical Research*, 109(DO1105), 1–11.

Witzke, R.L. and Bliss, T.J. (1950). Co-ordination of lightning arrester location with transformer insulation level. *Transactions of the American Institute of Electrical Engineers*, 69(2), 964–975.